

This article was downloaded by: [EPFL Bibliothèque]

On: 09 July 2015, At: 07:29

Publisher: Routledge

Informa Ltd Registered in England and Wales Registered Number: 1072954 Registered office: 5 Howick Place, London, SW1P 1WG



## Building Research & Information

Publication details, including instructions for authors and subscription information:

<http://www.tandfonline.com/loi/rbri20>

### Comprehensive annual daylight design through a goal-based approach

Siân Kleindienst<sup>a</sup> & Marilyne Andersen<sup>b</sup>

<sup>a</sup> Building Technology Program, Department of Architecture, Massachusetts Institute of Technology, Cambridge, MA, US E-mail:

<sup>b</sup> Interdisciplinary Laboratory of Performance-Integrated Design (LIPID), School of Architecture, Civil and Environmental Engineering (ENAC), Ecole Polytechnique Fédérale de Lausanne (EPFL), Lausanne, Switzerland

Published online: 21 Feb 2012.

To cite this article: Siân Kleindienst & Marilyne Andersen (2012) Comprehensive annual daylight design through a goal-based approach, Building Research & Information, 40:2, 154-173, DOI: [10.1080/09613218.2012.641301](https://doi.org/10.1080/09613218.2012.641301)

To link to this article: <http://dx.doi.org/10.1080/09613218.2012.641301>

PLEASE SCROLL DOWN FOR ARTICLE

Taylor & Francis makes every effort to ensure the accuracy of all the information (the "Content") contained in the publications on our platform. However, Taylor & Francis, our agents, and our licensors make no representations or warranties whatsoever as to the accuracy, completeness, or suitability for any purpose of the Content. Any opinions and views expressed in this publication are the opinions and views of the authors, and are not the views of or endorsed by Taylor & Francis. The accuracy of the Content should not be relied upon and should be independently verified with primary sources of information. Taylor and Francis shall not be liable for any losses, actions, claims, proceedings, demands, costs, expenses, damages, and other liabilities whatsoever or howsoever caused arising directly or indirectly in connection with, in relation to or arising out of the use of the Content.

This article may be used for research, teaching, and private study purposes. Any substantial or systematic reproduction, redistribution, reselling, loan, sub-licensing, systematic supply, or distribution in any form to anyone is expressly forbidden. Terms & Conditions of access and use can be found at <http://www.tandfonline.com/page/terms-and-conditions>

RESEARCH PAPER

# Comprehensive annual daylight design through a goal-based approach

Siân Kleindienst<sup>1</sup> and Marilyne Andersen<sup>2</sup>

<sup>1</sup>Building Technology Program, Department of Architecture, Massachusetts Institute of Technology, Cambridge, MA, US  
E-mail: sian.kleindienst@gmail.com

<sup>2</sup>Interdisciplinary Laboratory of Performance-Integrated Design (LIPID), School of Architecture, Civil and Environmental Engineering (ENAC), Ecole Polytechnique Fédérale de Lausanne (EPFL), Lausanne, Switzerland  
E-mail: marilyne.andersen@epfl.ch

Decisions affecting building form and orientation, and choices regarding opening size, type and positioning have a great effect on the building's access to daylight and are typically made during the earliest stages of architectural design. Computer simulations of daylight performance have become a powerful tool for making design decisions, especially since the diurnal and seasonal changes in daylight necessitate an annual, climate inclusive performance analysis because of the strong influence of climate conditions on daylight accessibility. However, the amount and complexity of information generated by an annual analysis can be overwhelming, so a need exists for appropriate, user-friendly methods to process and communicate these data to the designer. To address this problem, an alternative approach to traditional daylight analysis is explored here to develop appropriate goal-based metrics and annual graphic display formats which present illuminance, glare and solar heat gain data with a focus on time variations. Graphic outputs are created using the temporal map format to improve understanding of daylight performance as it varies over the year, and to enable comparisons to be made between spatial and non-spatial quantities. In particular, a consistent and intuitive triangular colour scale is proposed to express goal compliance, so as to enhance further comparability between dissimilar quantities and thereby assist with critical choices and performance tradeoffs during the design process.

**Keywords:** building design, building performance, daylight design, daylight simulation, glare, goal-based metrics, illuminance, solar heat gain, temporal maps

Les décisions affectant la forme et l'orientation d'un bâtiment et les choix relatifs à la taille, au type et au positionnement des ouvertures ont une grande influence sur l'accès du bâtiment à la lumière naturelle et sont habituellement opérés dans les toutes premières phases de la conception architecturale. Les simulations informatiques de la performance en éclairage naturel sont devenues un puissant outil de prise de décision en matière de conception, en particulier dans la mesure où les variations de la lumière naturelle au fil de la journée et des saisons nécessitent une analyse annuelle de la performance qui prend en compte le climat, vu sa grande influence sur l'accès à la lumière naturelle. Cependant, l'on peut être submergé par le volume et la complexité des informations générées par une telle analyse annuelle, de sorte qu'un besoin émerge pour des méthodes plus intuitives et adaptées pour traiter ces données et les communiquer au concepteur. Afin de remédier à ce problème, une approche alternative est explorée ici, visant à développer des techniques de mesures fondées sur des objectifs, et des formats de représentation graphique annuelle présentant les données relatives à l'éclairage, à l'éblouissement et à et aux gains solaires en mettant l'accent sur les variations sur le temps. Des visualisations graphiques sont créées, qui utilisent le format des cartes temporelles pour améliorer la compréhension de la performance lumineuse naturelle selon ses variations au fil de l'année, et pour permettre d'effectuer des comparaisons entre des données spatiales et non spatiales. En particulier, une échelle de couleurs triangulaire, constante et intuitive, est proposée pour exprimer une conformité aux objectifs, de façon à renforcer une comparabilité entre des volumes de données dissemblables et aider ainsi à opérer des choix cruciaux et des compromis de performance au cours du processus de conception.

**Mots clés:** performance des bâtiments, éclairage naturel, outils de simulation, éblouissement, techniques de mesures fondées sur les objectifs, éclairage, gains solaires, cartes temporelles

## Introduction

While the building sector accounts for over 50% of overall energy use in industrialized countries like Switzerland, lighting alone is responsible for almost one-quarter (on average 22%) of the electricity requirements in commercial buildings (Swiss Federal Office of Energy, 2009). Given that daylighting has also an immediate impact on heating and cooling loads (which, together with lighting, make up over half of a building's energy needs), the impact that efficient daylighting and solar control strategies can have on energy use is undeniable (Ihm *et al.*, 2009). On the other hand, numerous surveys have shown a strong preference for views and daylight against electric lighting (Heschong-Mahone Group, Inc., 2003; Boyce *et al.*, 2003) with, potentially, a positive impact on productivity and performance (Edwards and Torcellini, 2002; Heschong *et al.*, 2002; Rashid and Zimring, 2008) that could produce major financial returns. Recent findings in photobiology (Brainard *et al.*, 2001; Lockley *et al.*, 2006) also seem to favour an increased use of daylighting strategies from a health perspective because of its strong impact on circadian rhythms and hence on alertness, on the immune system and on sleep/wake states (Veitch, 2005; Webb, 2006).

However, all these benefits can only be achieved if daylight is properly controlled and managed so as to ensure both visual and thermal comfort. While decisions affecting the collection, transportation and distribution of natural light in a building are all made at different stages of the design process, not all decisions carry the same weight. Those that impact daylight access and collection will be the most influential on ultimate daylighting performance because they are the metaphorical first link in the chain. These include decisions made about building orientation, form, exterior shading, and window size and distribution, which are often addressed during the earliest stages of design.

Unfortunately, as several recent surveys have revealed, daylighting design explorations do not often happen during schematic design (Reinhart and Fitz, 2004, 2006; Galasiu and Reinhart, 2008). Furthermore, many architects are not taught to use daylight simulation software (Sarawgi, 2006) and tend instead to rely on experience, manual calculations and rules of thumb (Galasiu and Reinhart, 2008). Although this may work for simple, box-like spaces, the complexity of modern architecture begs a more computational approach to analysis and validation. Designers need

the education and resources to produce fast, unique design analysis which provide all information necessary to make decisions.

Where daylighting is concerned, there is not always a consensus regarding which information is 'necessary', but research has been moving towards annual climate-specific simulations. Daylight Autonomy (DA) (Reinhart and Walkenhorst, 2001) and Useful Daylight Illuminance (UDI) (Mardaljevic and Nabil, 2006; Mardaljevic, 2009) are two existing metrics that use annual simulations to find the percentage of time a sensor point is above or between given illuminance benchmarks. Another direction research has taken is graphing data as they change over time, such as in the temporal map format shown in Figure 1: colour-scaled surface graphs with year on the *x*-axis and day on the *y*-axis. This kind of representation is often generated together with spatial data so as to maintain information on how the light is distributed within the space. It is a powerful method for informing design decisions since interior daylight is heavily influenced by solar angles and climate conditions, which are themselves based on diurnal and seasonal cycles. This makes temporal graphics ideal for intuitively connecting design decisions with the ever-changing sources of daylight.

Only a few explorations into the use of temporal maps with daylighting data have been done, and unfortunately they still remain largely unknown to designers. Two studies of note include those by Glaser and Ubbelohde (2001) and Mardaljevic (2004). Both studies suggested that temporal data be displayed alongside spatial data, such as contour maps, sensor grids or false-colour maps, a combination now allowed by the recent developments in computer-based analysis and increasingly relevant to the needs of the design process (Reinhart and Wienold, 2010). Alternatives to numerical grids as spatial complements to temporal graphics are computer-generated renderings. This is the representation chosen in the proposed approach because of the appeal renderings have for designers, and their capability to provide both feedback on the spatial light distribution and an opportunity for qualitative assessment.

Regarding what *kind* of information should be given in annual datasets, the performance of daylight can typically be considered from three complementary perspectives (Reinhart and Wienold, 2010): illumination (usually derived from illuminance analyses), glare, *i.e.* contrast distribution (from different locations and

along different viewing directions), and overheating risks (associated with solar gains).

As these aspects of performance can often be conflicting and are linked to complex spatial and temporal relationships with the outside environment, it is very easy to get overwhelmed by information. Within the context of a design process, goal-based metrics have the potential to make this synthesis effort more straightforward. Such metrics would show how closely prescribed objectives are fulfilled rather than express absolute performance quantities. They thus offer the potential to format information in a way that directly makes sense for the project and for the designer ('am I (close to) achieving what I want?') without the intermediate step of interpreting the considered quantity itself.

This paper introduces three goal-based metrics for annual daylighting performance and a common format to display them graphically: a non-linear, triangular colour scheme applied to a temporal map format. The overall approach and colour scale are presented in the second section; the three metrics are described individually in the third to fifth sections; and their applicability as complementary information within a design process is discussed in the sixth section.

## Proposed framework for time-varied, goal-based daylighting metrics

### Complementing spatial daylight performance analysis

Daylight performance varies with both location and time. The simultaneous visualization of both dependencies would either result in one temporal map per point of interest within a space or in one performance data map at every moment in time. The second alternative is the one most commonly found in practice: displaying either instantaneous data (illuminance distribution, for example) for chosen moments (equinox and solstices at given times of day, for example), or cumulative data (DA distribution, for example) for the whole year. An attempt was made by Glaser and Ubbelohde (2001) to deal with the much less common first alternative through an intriguing 'brushing and linking' method: where the designer would move the cursor (via the mouse) over a representative location on the spatial grid of points and the adjacent illuminance temporal map would update accordingly. Conversely, the spatial grid of illuminances would update based on which moment in the temporal map the mouse was on. This method takes advantage of the computer's interactive capabilities, but the designer is still forced to analyse each point in space or each point in time separately.

For the sake of legibility, some form of summary is inevitable to avoid overwhelming the designer with

data. Such a summary allows the designer to quickly extract general trends of daylighting performance in the numerous fluctuations of external conditions. But it is inappropriate for software to impose *a priori* which, of space or time, is the more pertinent aspect to emphasize in a design process, as this will depend on the priorities of the project and the considered stage of design. Known metrics like, DA and similarly UDI choose to sacrifice an understanding of the time-based variability of performance in favour of retaining the spatial variability of performance. In other words, DA can show that for 70% of annual working hours, a particular point has adequate daylight, but it cannot show whether this point is underperforming in the morning hours, or in the winter.

Reversing DA's approach, a temporally based metric would condense the spatial variation to a single number while displaying variation over time. This alternative is interesting especially during the early stages of design where decisions regarding the orientation, position or sizing of openings and design of shading systems have to be made – all primarily driven by daily and seasonal variations – and where the specifics of space use may still be somewhat undefined, which would make a spatial summary acceptable or even pertinent. Before discussing what this metric or set of metrics should be, there is a need to define a simulation framework in which such metrics could be produced so that the results can be visualized in a synthetic way.

### Producing and displaying annual daylight data

Although annual datasets are the only way to provide the designer with a complete picture of daylighting performance, the simulation of annual light levels can be computationally intensive. The temporal map shown in Figure 1 was created using over 100 000 illuminance values at a single sensor point generated by the program Daysim for 5-min intervals and relying on the daylight coefficients method to speed up the process (Reinhart, 2005). To pre-process annual data and reduce the necessary number of simulations, a method was developed by the authors to condense hourly weather data within a limited number of adjacent time periods to represent a year (Kleindienst et al., 2008). This method produces a limited yet representative set of renderings and temporal data for the year, which provides support for design decisions equivalent to what a high-resolution analysis would provide.

The method works as follows. First the year is divided into annual and daily periods of similar solar angles: the number of divisions used to represent the changing nature of daylight is seven daily divisions and eight annual divisions, for a total of 56 annual periods. Each period is processed using a method based on the

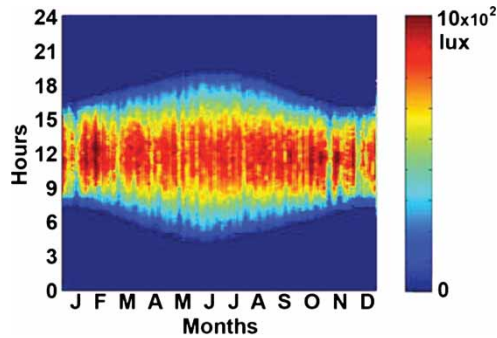


**Figure 1** Temporal map displaying illuminance data using a colour scale. The x-axis represents the year; the y-axis represents the day

ASRC-CIE sky model (Perez *et al.*, 1992), from which a reduced set of realistic renderings is generated. For instance, four illuminance simulations are done under clear, clear-turbid, intermediate and overcast skies of average brightness for the year and time period, and the results of these simulations are then summed and weighted by the frequency of that sky type's occurrence. If data are pre-processed appropriately, the benefit of such a method is that the responsibility of choosing which moments and weather conditions should be simulated is lifted from the user, who can instead benefit from a comprehensive presentation of annual performance.

Although 56 annual periods is sufficient resolution to show changes in diffuse light, it is not enough to represent direct sun in a more complex situation such as with sun access restricted to small sky areas that might not include one of the 56 (or, really, 28) considered sun positions (Kleindienst *et al.*, 2008). A further refinement of this data-reduction method has thus been developed here; it first calculates the diffuse illuminance trends for the 56 averaged periods described above, then overlays the direct sun contribution at 1200 moments for which an additional zero-bounce sun penetration calculation

is performed (discarding interior reflections). Only when the new illuminance exceeds the original value at that point on the temporal map (which would show that a direct sun penetration situation has indeed been missed) will the overlay actually be applied. Figure 2 shows an example of a detailed temporal map produced using Daysim (similar to Figure 1), as well as the equivalent map produced using the data-reduction method with sun overlay. It is reasonable to assume that this refinement will suffice to capture sun dynamics adequately, as it catches more direct sun contributions than Daysim – based on contributions from 60 to 65 sun angles during the year (Reinhart, 2005) – or than the new DDS scheme described by Bourgeois *et al.* (2008), who propose 2305 direct daylight coefficients evenly distributed over the full sky dome (whereas the proposed 1200 points are concentrated within the actual sun angles of a location's specific path).

### Goal-based metrics in the design process

When one performs a daylighting analysis during the early design stages, it is implicitly or explicitly to test the extent to which a design intent meets one's expectations or performance objectives (and if not, to test alternatives that would). These objectives are sometimes very well defined and specific (illuminance targets for code compliance, for example), sometimes less so (fulfillment of a general design intent). Generally speaking, the overall objective is to get closer to a given target. However, these quantities are very different in nature: illuminance is typically assessed over a spatial grid; glare has to be evaluated from given viewpoints within the space; and solar gains is a non-spatial quantity, usually evaluated for a whole space or building.

These different aspects of daylighting performance must, however, be assessed together, so that design efforts and (probable) compromises can be done with a holistic perspective. A goal-based approach thus appears as a very straightforward way to get them to

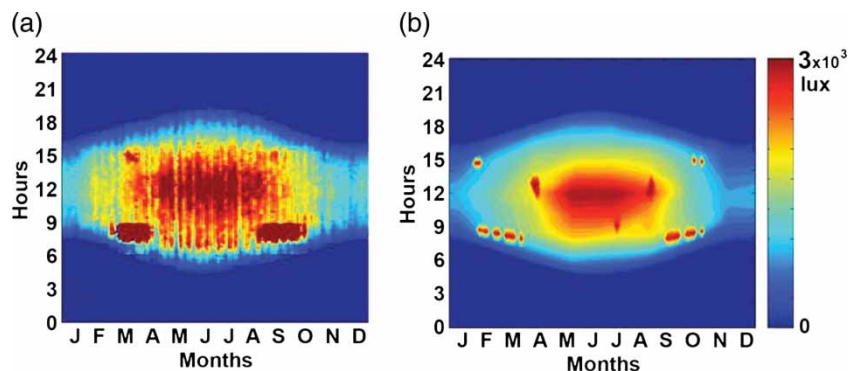


**Figure 2** (a) Detailed temporal map produced using Daysim's output illuminances and (b) a temporal map produced using the 56 annual periods method

become comparable: what is then being compared is always how closely they each fulfil their respective objectives, even though the measured or calculated quantities used to evaluate this can greatly differ amongst them. A consistent value scale for such an approach is presented in the next section.

At the early design stage, it is also likely that some programmatic aspects are yet to be defined, which would shift the evaluation needs towards ‘perimeters’ of interest within a space, rather than specific locations (*e.g.* ‘back of the room’ or the ‘desk area’). A goal-based metric that could provide a synthetic value for such customized perimeters of interest would enable a high-level analysis, particularly pertinent when exploring early design options. It would also make comparisons between alternatives more straightforward as a single value would have to be compared instead of a grid of values (spatial distribution).

A set of three metrics is proposed to answer these constraints. First, an illuminance-based metric, which displays the percentage of an area of interest that stays within a chosen lux range, and is referred to as Acceptable Illuminance Extent (AIE). Second, a similar approach using a single number to represent overall glare perception within an area of interest, introduced as Glare Avoidance Extent (GAE). To be realistically applied, it requires more efficient methods for computing glare. Third, a new metric called Solar Heat Scarcity/Surplus (SHS) was used to convey the urgency of either allowing more direct solar gain or avoiding it. It is based on revisited balance point calculations.

The proposed approach deliberately does not assign actual goals for each metric. Instead, it provides a framework in which the designer can set the goals. These goals are sometimes chosen freely (*e.g.* for minimum and maximum illuminance thresholds), sometimes selected amongst predefined criteria (*e.g.* for glare perception), or based on external conditions as for solar gains. The designer decides what goals are appropriate – and how loose or strict these objectives should be – based on code or on other project priorities that might actually exceed strict daylighting performance. He or she can then use the generated analysis results to guide him/her closer to these objectives or, perhaps, to choose more reasonable goals.

### **A consistent, non-linear colour scale for goal-based metrics**

The temporal map format introduced above is used to display the three mentioned goal-based metrics. Whatever the goals are, a consistent scale to express goals fulfilment should be maintained in order to allow the user to visualize easily how far the design currently is from reaching the goals. The colour-based information

is displayed on temporal maps to preserve the variability of diurnal and seasonal performance.

For all three metrics, there are at most three possible outcomes: either data fall within the desired range, or they exceed the maximum, or they do not reach the minimum. To maintain this information intact on a single graph, the temporal maps shown here use a triangular rather than a linear colour scale (Figure 3). In the triangular scale, yellow represents data that have met the designer’s goals, blue represents data that are too low, and red represents data that are too high. Following from this, orange represents a moment when part of the data is too high and the rest acceptable; while greenish is used for a moment when part of the data is too low. Purple, therefore, represents a moment when the data include both high and low values, such as in a dim room with direct sun spots. Any colour within the triangle is thus a possible outcome.

The sample temporal maps shown in Figure 4 illustrate the interpretation of colour. The three displayed colours represent not raw data, but goal compliance for any metric, which makes it easier to understand tradeoffs between dissimilar metrics. For instance, while illuminance, glare and solar gains are measured in very different ways (as discussed in more detail in the following sections), goal compliance can directly be compared between metrics and the designer can thus gauge the effects of optimizing for one performance over another: in all graphs, yellow will consistently indicate compliance with goals, red will always indicate exceeding goals and blue will indicate falling short of goals, within user-defined areas of interest.

The specific chosen colour pattern seems very intuitive for people to understand, based on user studies and tool feedback received so far (see the sixth section). A refinement of the colour gradation might still be beneficial, *e.g.* to better distinguish blue from purple. A study of how colour patterns are most efficiently perceived by eye will thus be envisaged in the future.

### **Lightsolve context**

The graphical formats and concepts presented in this paper are being applied to a new design tool called Lightsolve, which is under development by the authors and specifically focuses on the exploratory, early-stage of design (Andersen *et al.*, 2008, 2011). Currently using computer-aided design (CAD) inputs from SketchUp, it performs a representative group of hybrid radiosity and shadow volumes simulations using the LightSolve Viewer (LSV) engine (Cutler *et al.*, 2008) based on TMY2 weather files, and graphically displays the results as temporal maps and spatial renderings. Figure 5 shows the main features of the

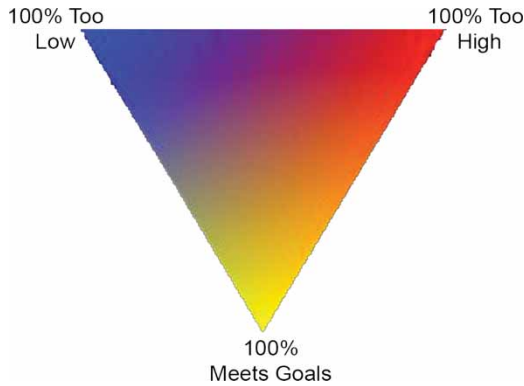


**Figure 3** Triangular colour scale for goal-based metrics: yellow = 100% meets goals; blue = 100% too low; and red = 100% too high

Lightsolve interface, in which the renderings update when the user scrolls over the temporal maps, similar to the ‘brushing and linking’ method described by Glaser and Ubbelohde (2001, 2002), but here based on goal-based metrics applicable to entire areas of interest and linked to renderings. In this way, the user can interactively connect the time-based performance of the space with a realistic rendering of sun penetration and light distribution for a single weather type, or for the dominant conditions at that particular period of the day and year.

### Illuminance analysis based on user-defined thresholds and areas of interest

To represent time-varied performance on a temporal map, calculated illuminance values first need to be processed into a metric that efficiently conveys the information the designer seeks. A new metric was developed that reports the per cent of an area of interest that stays within a user-defined illuminance goal range, which is far preferable to any averaging method that could potentially hide a combination of

extremes behind a reasonable average number. It is conceptually similar to the UDI metric (Mardaljevic and Nabil, 2006; Mardaljevic, 2009) in that it applies a lower and an upper threshold, but it has fuzzy boundaries and, more importantly, it relates to a whole perimeter of interest, as detailed below. This metric, in essence, defines the amount of space that stays within acceptable limits, so it is called the AIE.

### Illuminance metric principle

The main idea of AIE is to pre-process spatial illuminance data in terms of given design goals. Though AIE goals are basically for the designer to determine, default lower values will often correspond to prescribed codes or other benchmarks based on space use (Rea, 2000; US Green Building Council (USGBC), 2009), and upper thresholds to space-specific recommendations (avoidance of too high cumulative exposures in museums, for example, whereas a circulation space might not need an upper threshold at all).

Once the threshold values are chosen, AIE can be calculated as follows: given an array of illuminances over an area of interest (AOI), the number of sensor points (or sensor patches in the case of radiosity-based calculations) that fall within the desired range is determined, as well as the number of sensors where illuminances were too high or too low. The per cent of total sensors that fall within the goal range is the AIE. And the corresponding temporal map shows how much of any given area of interest falls within the desired range, using the colour scale described in the previous section: yellow (100%) if the entire area falls within the target range at that period of year and time of day; and a redder or bluer hue the more of the area falls above or below it.

In reality, illuminances that fall outside the prescribed range may still have value; it is difficult to argue that one cannot read just as well with 390 lux as with

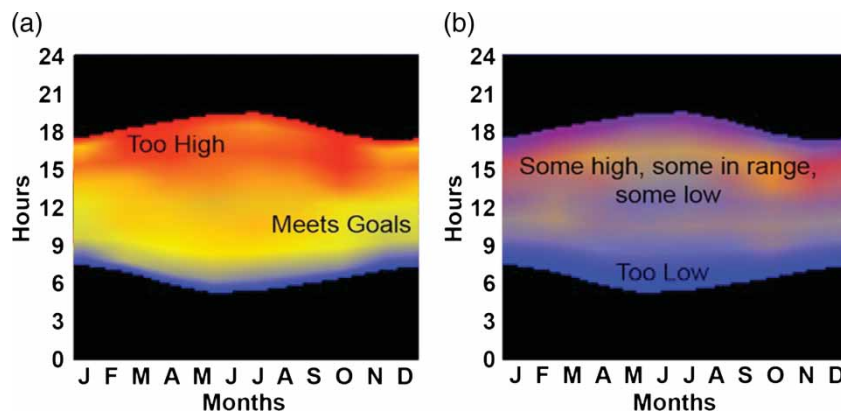


**Figure 4** Demonstration of triangular colour scale interpretation

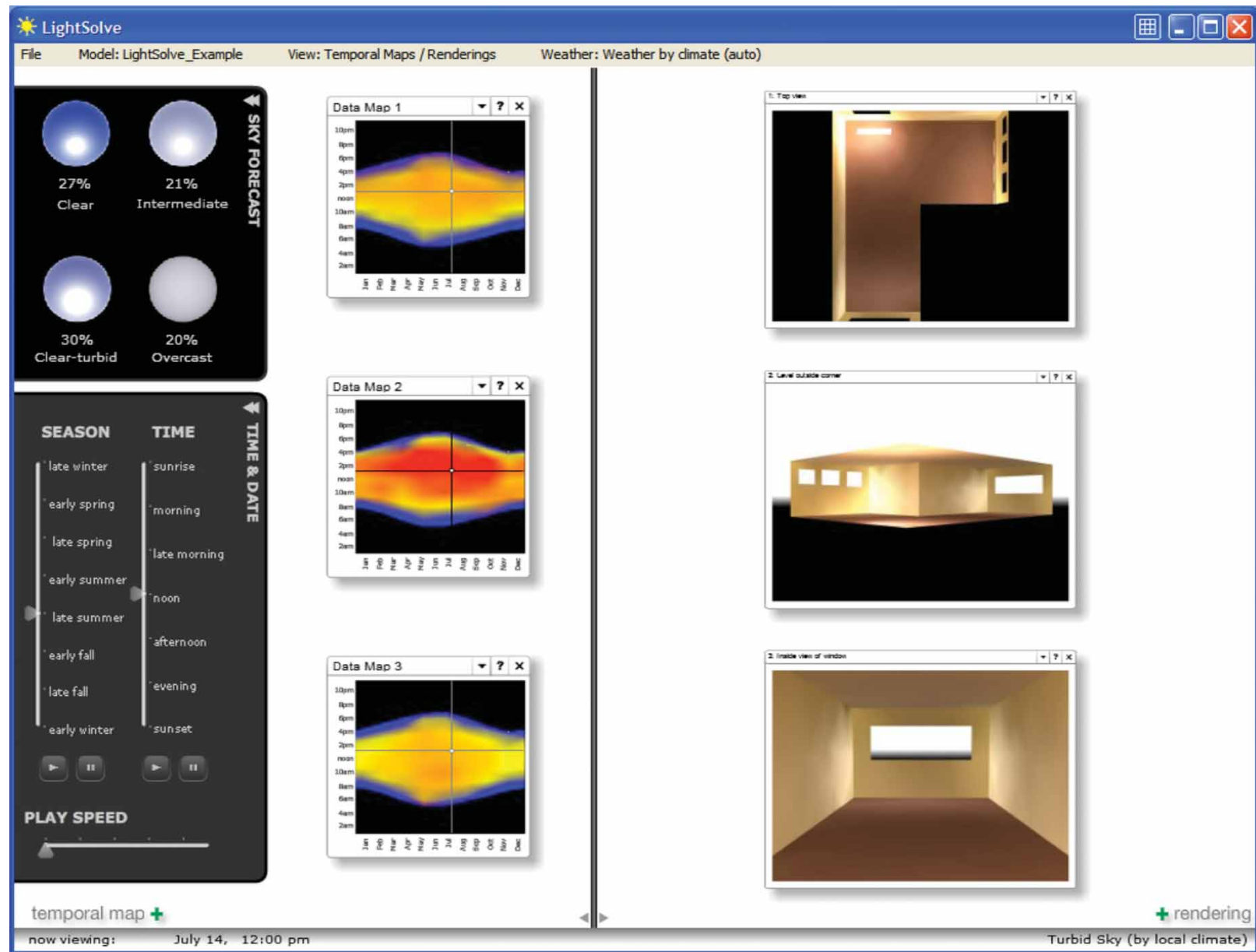


Figure 5 Lightsolve interface displaying both temporal maps and related spatial renderings



400 lux, and from this perspective a hard cut-off seems unreasonable. For this reason, Rogers (2006) developed the Continuous Daylight Autonomy metric, which gives partial credit for all illuminances less than the minimum threshold. For AIE, a ‘buffer zone’ can also be applied, so that models with many sensors reading just below the minimum threshold do not generate the same results as those in which the sensors are far below that limit.

The upper and lower buffer zones can again be any size (although the minimum buffer illuminance cannot be below zero), and they do not have to be the same size as each other. Their width will depend on the designer’s goals for the project and should represent four tipping points (*i.e.* four threshold illuminance levels): the level below which daylight is not even useful (acceptable low threshold), the level above which illuminance is satisfactory for the considered perimeter (desired low threshold), the level below which it is still satisfactory (desired high threshold), and the level above which daylight should be avoided (acceptable high threshold). Figure 6 shows how partial credit can be applied on a linear scale for sensors that fall between the buffer threshold and the actual threshold.

#### Application example

Figures 7 and 8 illustrate how this metric can inform about the daylight performance of two iterations of a simple classroom model. The model is located in Sydney in New South Wales, Australia, and given an illuminance range goal of 400–1000 lux on the work plane (with partial credit given down to 200 and up to 2000 lux); the illuminance thresholds in this example were inspired from the fact that illuminance values above 200 lux are generally accepted as being useful and above 300–400 as optimal for classrooms. Levels above 1000 lux and certainly above 2000 lux may create contrast levels that are too high (Saxena

*et al.*, 2010). No occupancy hours are given for this model, so all sunlight hours are relevant here. The room is 7.5 × 10 × 3 m high, with the short facade on the north and south faces. All surfaces are greyscale; and opaque surfaces are lambertian. The ceiling reflectance is 83%; the wall reflectance is 65%; the floor reflectance is 20%; and the visible transmittance of the glass is 80%. As it is a classroom, there is a 6 × 1.5 m chalkboard on the east wall with a 5% reflectance. Radiance was used to perform the rendering and illuminance measurements at nine workplane sensors, and the rendering parameters used were: -ab 5, -ar 128, -aa 0.1, -ad 2048, -as 256, -dp 1024, -ds 0.15, -dt 0.05, -dc 0.75, -dr 3, -ms 0.066, -sj 1, -st 0.01, -lr 12, -lw 0.0005, -I +, and -h.

In the first iteration (Figure 7), the blue at the temporal map’s edges indicate that not enough light reaches the space at the extremes of the day; and yellow (tinged with orange) in the midday of the colder half of the year denotes that the illuminance levels meet the goals, with some higher sun spots. During warmer days, however, purple indicates that part of the room remains too dark, while part of it remains too bright. This may be due to the shorter penetration of summer sun angles, which would bathe the front of the room in bright sunlight while leaving the back of the room dark, an assumption the designer could easily verify by looking at the corresponding renderings in Lightsolve (cf. Figure 5). The second iteration (Figure 8) has added an overhang and a light shelf to the north windows shifted up, and has introduced two small windows on the south side. The combination of bilateral light and sun shading has reduced the instances of both high and low illuminances, so that most of the temporal map (*i.e.* most of the year) shows yellow, or ‘in range’.

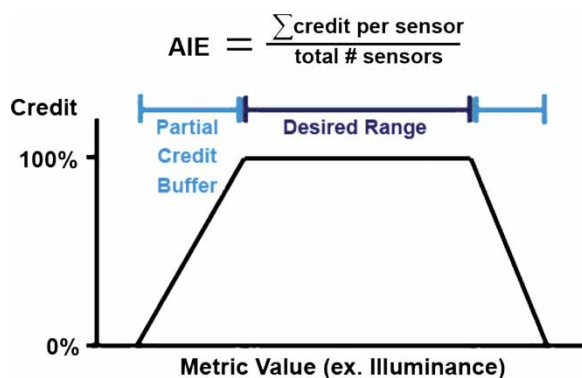


**Figure 6** System of credit and partial credit for AIE. Values within the desired range get full credit; those in the buffer zone get partial credit

#### Glare analysis over perimeters of interest

The glare metric used as a basis for the proposed method is the Daylight Glare Probability (DGP). It is one of the most promising and best validated metrics for daylight glare and was developed by Wienold and Christoffersen (2006) from user surveys conducted under real daylight conditions.

Although fast annual illuminance calculations are possible through the daylight coefficients method (Tregenza and Waters, 1983) or the time-segmentation method described above, *e.g.* if the annual glare potential is to be determined, then the calculation intensity becomes an issue due to the associated rendering and pixel processing required by most full-glare analyses.

Because the program written to calculate DGP, *eval-glare*, involves the pixel analysis of Radiance

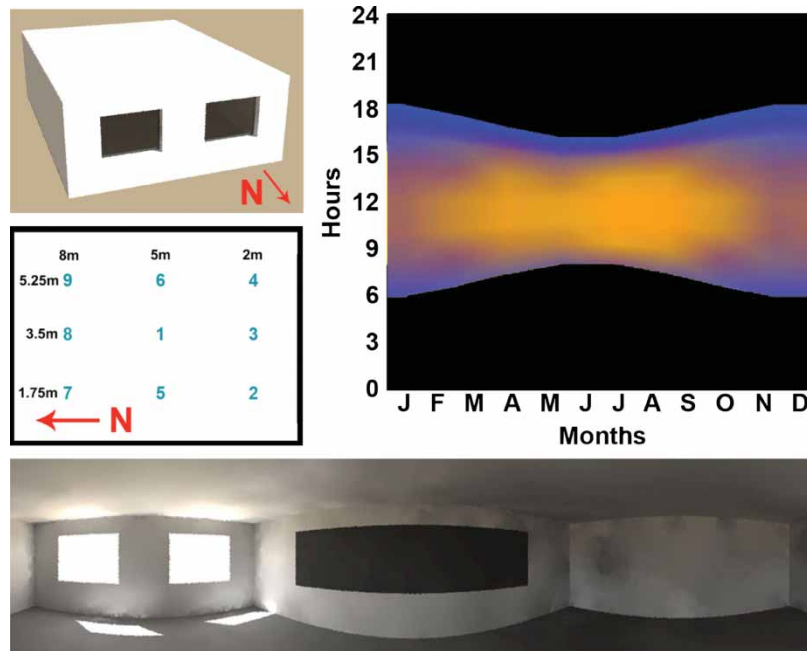


**Figure 7** Cylindrical interior rendering (bottom), exterior rendering (top left), point diagram (middle left) and temporal map of the work plane AIE (top right) for iteration 1 of a simple model

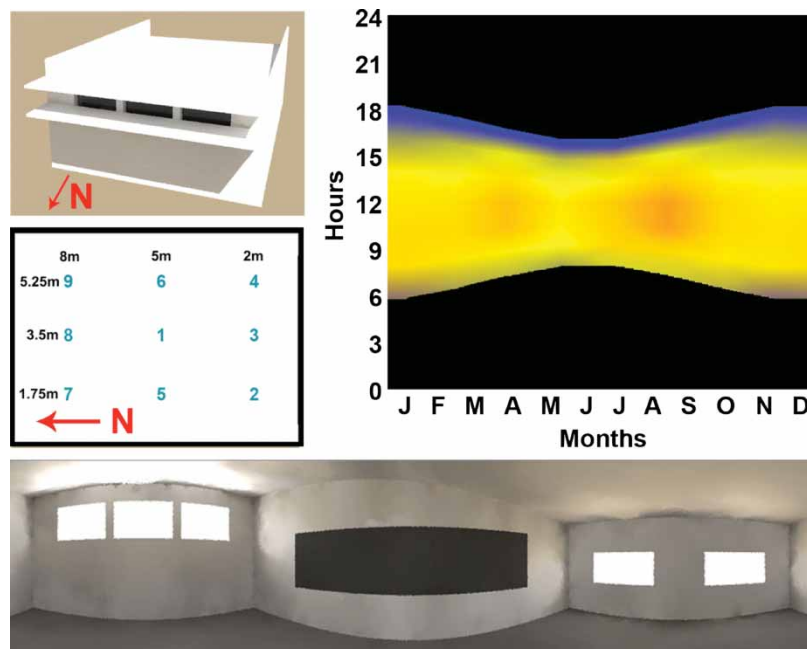


**Figure 8** Cylindrical interior rendering (bottom), exterior rendering (top left), point diagram (middle left) and temporal map of the work plane AIE (top right) for iteration 2 of a simple model

renderings, Wienold (2009) developed an approximation method called the simplified DGP, or DGPs to improve the computational efficiency for annual calculations. It takes the form of a linear equation depending only on vertical illuminance, but is applicable only when there is no direct solar

contribution and when a combination of rather high illuminance and low contrast is ensured. Another attempt to reduce the calculation intensity of glare was developed for DOE-2 in the 1980s. Winkelmann and Selkowitz (1985) used internal illuminances and known building geometry to find glare at given

reference points using Hopkinson's Glare Index equation. This method was validated only within 15% of the results derived from the program SuperLite and from physical model simulations, both modelling tools also of low demonstrated accuracy (Ubbelohde, 1998; Cannon-Brookes, 1997; Thanachareonkit *et al.*, 2005), but it still provided an interesting modelling framework from which to build upon, briefly introduced by Kleindienst and Andersen (2009a). The proposed method attempts to improve on the weaknesses of the DGPs while using information from an input model's geometry and materials, without the need for any renderings or non-illuminance simulations. This approximation is referred to here as the DGPM because it is a model-based DGP approximation.

### Model-based approximation for glare calculations

The DGPM approximation is calculated using the Lightsolve rendering engine (Cutler *et al.*, 2008), which stores geometry as a triangular meshed object file. To jumpstart glare source identification, therefore, every triangular glass patch is assumed to be a possible source of glare. For each glass patch, geometric quantities such as the position index and the angular patch size can be determined from the object file. The luminance of the glare source is defined by the luminance of the sky behind the glass patch, weighted by the transmissivities of any object the line of sight passes through (Figure 9). Diffuse luminances for the sky are found using Commission Internationale de l'Éclairage (CIE) sky models (CIE, 1994), while sun and ground luminances are based on the equations used in Radiance (Ward, 1998). The sun, if it appears through any glass patch, is treated as a separate glare source. An annual set of vertical illuminances is found using the data-reduction method and the high-frequency direct sun contribution overlay described in the second section. Note that because the data-reduction method used to find annual illuminances involves a weighted sum of the illuminances simulated under four discrete sky types, the DGPM should be calculated *before* this weighted summation is performed: the vertical

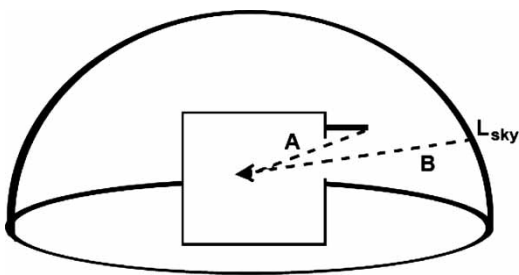


**Figure 9** Transmissivity weights: line A is zero luminance, as it is stopped by an object with zero transmissivity; line B is weighted by the transmissivity of the window glass

illuminance and the sky dome luminance are both included in the DGP equation, so the relationship must be kept intact to find an accurate DGPM. This way, the DGPM will represent glare resulting from a real sky condition.

Four models were used to validate the DGPM method against the DGP found using the program Evalglare, and the same validation process was performed using the DGPs equation as a comparison. These models were chosen to cover a range of situations, including a well-lit room with large vertical windows (for which the DGPs method should be well suited), a room with skylights instead of vertical windows, and two rooms with smaller openings and darker walls and frames. The latter two (one of which is illustrated in Figure 10) were meant to represent situations where low-illuminance contrast-glare dominates. In each case, the DGPM method performed as well as or up to 20% better than the DGPs method, most notably in the three cases with either skylights (rather than vertical windows), or with low illuminance, contrast-based glare scenarios.

### General versus maximum glare potential

Similar to illuminance simulations, analysing glare moment by moment and view by view would give a disjointed picture of the whole performance and would make analysis unnecessarily complicated. Fortunately, with the proposed approximation relying only on illuminance simulations and geometric information, annual DGP can be simulated as quickly as annual illuminance data.

From this point, there are two directions in which one can go, and both options should be made possible. The DGP values for each period of the year can be, like the annual illuminance values in the data-reduction method, weighted according to the frequency of each sky type. Alternatively, the maximum glare value among the four sky types could be selected to represent each time period. The former method would indicate the likely glare occurrence as dictated by local climate, while the latter would be a type of worst-case scenario. This worst-case logic could be even extended from temporal to spatial variation by taking the maximum glare perceived by any sensor point. This would be useful in situations where no glare can be tolerated.

Finally, it is likely that a designer is concerned about glare within defined areas of interest (potentially the whole room), not just in selected positions and view directions. In the earliest stages of design, the programmatic layout of a space may not be fully defined, making the important locations and view directions uncertain. Like AIE, drawing all related data points into one graph reduces the mental processing required to understand multiple graphs while drawing out

general trends, and making the data concise and readable. The proposed metric, called GAE, is goal based and defined as the portion of glare sensors whose associated DGP value is less than a certain threshold.

### Design goals for daylight glare probability

The most common design goal for glare is to avoid it completely. At the very least, the designer should be told when glare occurs, so the DGP data points should be categorized according to DGP thresholds indicating glare perception. Wienold (2009), who developed the original DGP metric, indicates that 35%, 40% and 45% DGP are reasonable thresholds for ‘perceptible’, ‘disturbing’ and ‘intolerable’ glare, respectively.

A point representing less than 35% DGP would be given ‘full credit’ for avoiding glare, which in the AIE analogy is equivalent to being within the prescribed illuminance range. Above 35% DGP, at which glare becomes ‘perceptible’, the scale of credit decreases until it hits zero at 45% DGP, after which there is no credit given for avoiding glare because it has become ‘intolerable’.

On a temporal map, a large number of sensors perceiving glare would appear as oranges and reds, or ‘too much glare’ in the goal-based lexicon. Yellow with very little orange in it might represent a lot of sensors perceiving ‘just perceptible’ glare, or a few sensors perceiving ‘disturbing’ or even ‘intolerable’ glare.

The option is purposely left to the designer to group glare sensor planes according to the information desired as this will vary according to the project and the intended use. For instance, in a classroom model, with all desks facing the same direction, the designer might set up an array of vertical sensor planes at a seated student’s head height facing the chalkboard (Figure 11a). On the other hand, if the designer wants a more general understanding of the glare potential in a space, an array of sensors facing in several different directions could provide that view (Figure 11b). The most useful view directions to model would be those that are directly normal to windows.

The climate-based scenario for both temporal and spatial variation is the one demonstrated in Figure 12, while in a more sunny climate or in a situation where glare should absolutely be avoided, the maximum glare scenario should be chosen. The DGPm values for each period were made into a weighted sum according to sky type occurrence, and the value represented on the temporal map represents the per cent of sensors that do or do not perceive glare. The model is based on Tadao Ando’s Church of Light in Osaka, Japan, and the glare sensors are set up in rows facing the narrow cross-shaped window at the front of the church.

### Solar heat gain desirability

Even though solar heat gain is not a photometric quantity, it is one of the significant tradeoffs associated with daylighting, and therefore it should be considered in any holistic analysis of daylighting. Most existing daylighting analysis solutions that include solar heat gain are those that either include or have easy exports to energy analysis tools (Urban and Glicksman, 2007; Reinhart *et al.*, 2007). The few existing analysis methods that do not require simulation are usually only applicable to certain restricted climate locations and use the existing results from previous energy simulations in their application (de Groot *et al.*, 2003; Hui, 1997). Very few of these methods or tools parse the solar heat gain contribution out from the general energy analysis and present it separately as a trade-off to incoming daylight (de Groot *et al.*, 2003).

Focusing on the specific contribution of solar gains, the approach adopted here uses a simple (and existing) energy balance equation – the balance point method – to generate a solar heat gain metric similar in form to the AIE and GAE metrics discussed in the third and fourth sections. This metric, named Solar Heat Scarcity/Surplus (SHS) and briefly introduced by the authors in a conference paper (Kleindienst and Andersen, 2010), provides an indication of the urgency for shading windows during the cooling season or allowing more solar gain during the heating season.

### Balance point energy analysis exploration

A building’s balance point is defined as:

the outdoor air temperature required for the indoor temperature to be comfortable without the use of any mechanical heating or cooling.  
(Utzinger and Wasley, 1997)

It can be graphed in opposition to the outdoor temperature over the course of a day for an immediate visual representation of heating and cooling load potential (Figure 13).

Although it is a simple energy balance, the balance point equation still requires some user inputs. Envelope areas can be found automatically from the model geometry, and solar gain penetration through windows can be calculated using daylighting simulations. However, thermal resistance of the building envelope, ventilation rates, occupancy and internal heat gains need to be specified by the user. In the context of a daylighting tool, the authors envision drop-down menus with editable defaults based on building type. The biggest limitation of the balance point method is that it is steady-state and does not account for thermal mass effects.

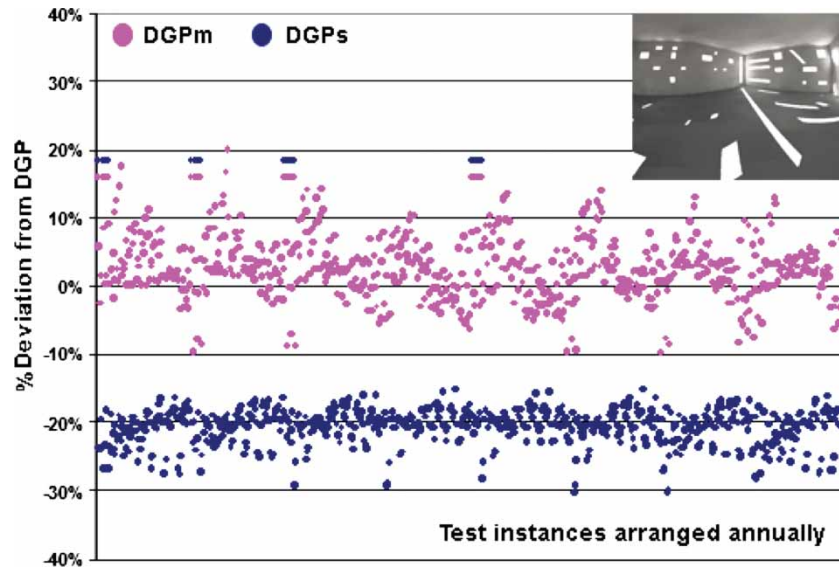


**Figure 10** One of the low-illumination models used to test the DGPm. The pink points represent the deviation between DGPm and full DGP; blue represents the deviation between DGPs and full DGP

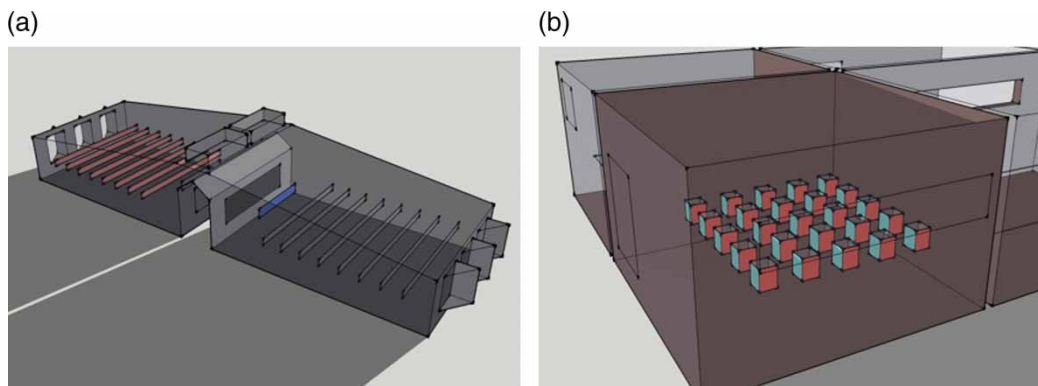


**Figure 11** (a) Classroom model in which glare arrays have been set up at student head height and single planes at teacher head height; and (b) an array of glare sensors, each face pointing to a cardinal direction

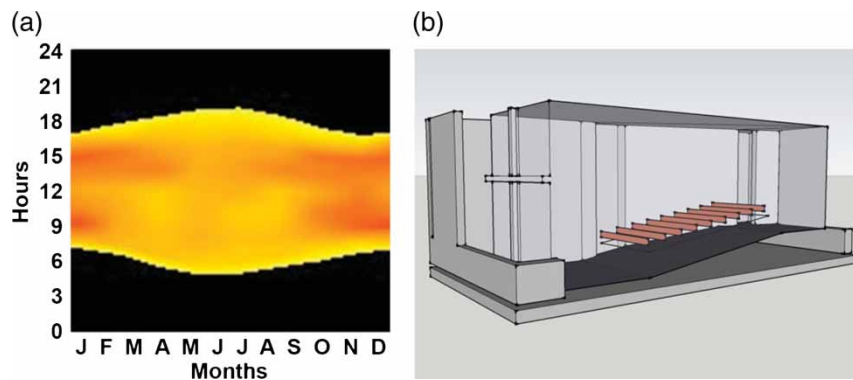


**Figure 12** (a) Temporal map showing GAE; and (b) CAD model inspired by Ando's Church of Light in Osaka, Japan

To explore the possible errors of the balance point method, balance point-calculated loads were compared with Energy Plus-simulated loads using the 16 commercial benchmark buildings released by the

U.S. Department of Energy (DOE) (Torcellini *et al.*, 2008). Two types of balance points were calculated: one using the complex occupancy and equipment schedules of the Energy Plus models, the other using a much

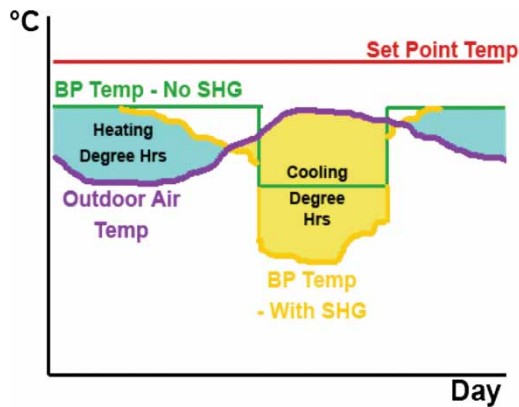


**Figure 13** Schematic diagram of how to find heating and cooling degree-hours by comparing balance point temperatures with the outdoor air temperature

simplified schedule. Because the continuous spectrum of loads crosses the zero line between cooling and heating, where small differences in load can cause huge errors, a maximum load ratio was considered rather than the absolute error. This means that the difference between balance point and simulated energy use was compared with the annual maximum heating or cooling energy use, whichever was more appropriate, and this comparison was nicknamed the maximum load ratio (MLR). The average MLR for the 16 buildings simulated in 16 cities were visually divided into categories of correlation in Figure 16 to aid in understanding the results.

The graph in Figure 14 shows the correlation level of building and climate locations with a very good MLR correlation; Figure 15 shows a very poor MLR correlation. The very poor correlation represents the large hotel, which is one of the three largest, and therefore more thermally massive, buildings in the benchmark set of 16 commercial buildings. The bar graph in Figure 16 illustrates the spread of correlation results for the detailed balance point calculation and the simple balance point calculation. The majority of daily load totals fell within 30% MLR ('good' or 'very good'), and those that did not were generally high-mass buildings or buildings with very complex schedules. The definition of correlation categories was based on visual groupings of graphs similar to those shown in Figures 14 and 15.

#### A two-part solar heat gain indicator

Using the balance point analysis described previously, a building could be said to have excessive solar gain when the outdoor temperature is greater than the building balance point and be lacking in solar gain when the outdoor temperature is lower than the balance point. The 'right' amount of solar gain

would be how much is required for the outdoor temperature to equal the balance point.

To apply the above reasoning mathematically, the proposed solar heat gain metric is split into two parts, called Solar Heat Scarcity and Solar Heat Surplus or SHS in both cases based on whether heating or cooling is required by the building:

$$\text{If } T_{\text{out}} - T_{\text{SHG+IHG}} \geq 0 \rightarrow \text{Solar Heat Surplus (cooling)}$$

$$\text{If } T_{\text{out}} - T_{\text{SHG+IHG}} < 0 \rightarrow \text{Solar Heat Scarcity (heating)}$$

$$\text{Solar Heat Surplus (cooling)} = 2 \times \left( \frac{T_{\text{IHG}} - T_{\text{SHG+IHG}}}{T_{\text{set}} - T_{\text{IHG}}} \right) \times \max \left[ \left( \frac{T_{\text{out}} - T_{\text{SHG+IHG}}}{T_{\text{IHG}} - T_{\text{SHG+IHG}}} \right), 1 \right]$$

$$\text{Solar Heat Scarcity (heating)} = \frac{-(T_{\text{SHG+IHG}} - T_{\text{out}})}{T_{\text{IHG}} - T_{\text{out}}}$$

where  $T_{\text{SHG+IHG}}$  is the balance point temperature ( $^{\circ}\text{C}$ ) based on both solar (SHG) and internal (IHG) heat gain;  $T_{\text{IHG}}$  is the balance point temperature ( $^{\circ}\text{C}$ ) based only on internal heat gain (IHG);  $T_{\text{set}}$  is the heating or cooling thermostat set point ( $^{\circ}\text{C}$ ); and  $T_{\text{out}}$  is the outdoor temperature ( $^{\circ}\text{C}$ ).

Solar Heat Scarcity ranges from 0% to -100% and is the percentage of the heating load *not* offset by solar gain (Figure 17c). Solar Heat Surplus is based on the same idea. It ranges from 0% to 100% and is partially defined by the per cent of solar heat gain that needs to be eliminated to bring the cooling load to zero, with a maximum value of 100% (Figures 17a and 17b). However, because the balance point-based cooling load often exceeds the load due only to solar heat gain, if Solar Heat Surplus was defined using this simple equation, it would too often saturate at 100% and lead to the (potentially wrong) conclusion that too much solar gain is allowed in the space: the reason for a 100% value might instead be that internal gains are very high. Therefore, the proportion of overall gains that are actually attributable to solar gains must become an explicit parameter in this equation. The weighing factor for this parameter should be large enough so that the metric benefits from most of the 0–100% range in all but the extreme situations, but small enough not to dominate the equation. It was found that a factor of two fulfilled both conditions, which led to the equation above. As a result, buildings with large internal loads may get a low Solar Heat Surplus value even though cooling loads are high. This makes sense because these loads are not for the most part attributable to solar gains, so decreasing the latter would not really help anyway.

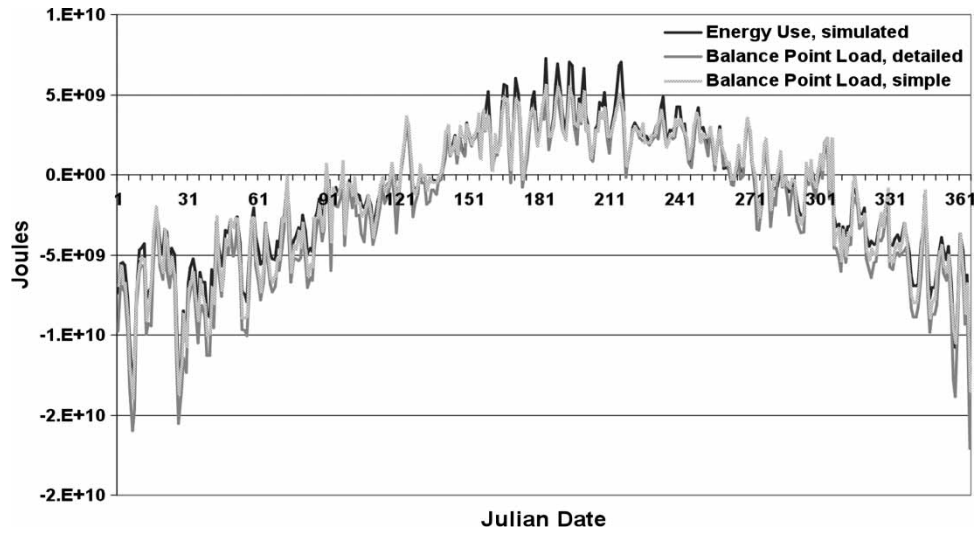


**Figure 14** Annual variation in Energy Plus-simulated energy use and the two calculations of balance point load showing good MLR. Retail model, Chicago in Illinois, US

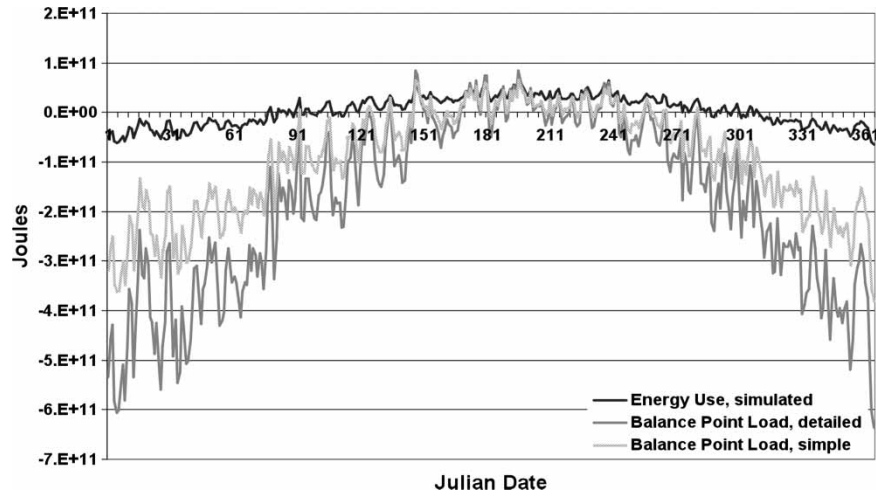


**Figure 15** Annual variation in Energy Plus-simulated energy use and the two calculations of balance point load showing poor MLR. Large hotel model in Minneapolis, Minnesota, US

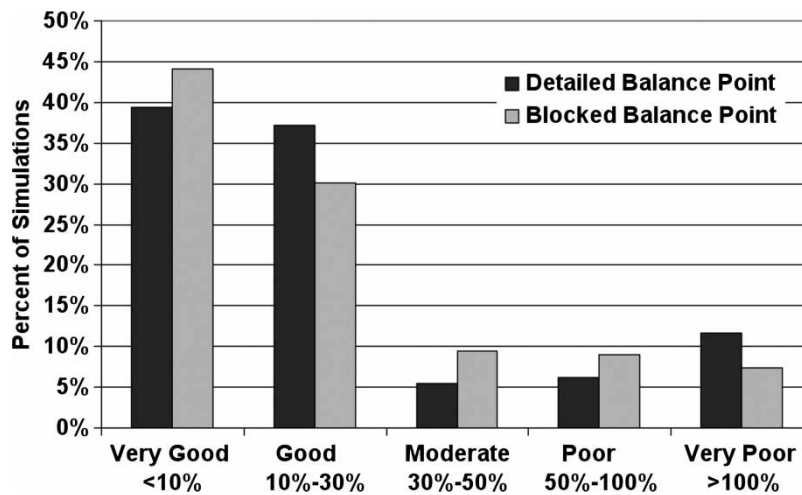


**Figure 16** Spread of maximum load ratios between Energy Plus data and balance point calculations for all simulations

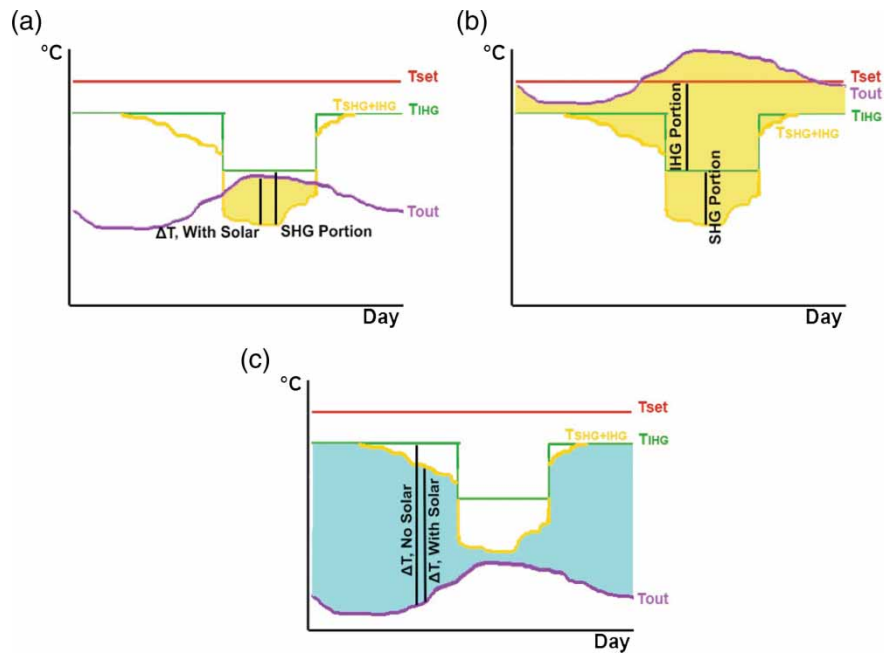


**Figure 17** Schematic examples of (a) solar heat surplus where the cooling required is less than the solar heat gain alone; (b) solar heat surplus where required cooling exceeds solar heat gain effects; and (c) solar heat scarcity

### Graphing SHS based on calculation resolution

For both Solar Heat Surplus and Solar Heat Scarcity, i.e. for SHS in general, the closer a value is to 0% the better, because 0% SHS represents the perfect amount of solar heat gain to match the building balance point and the outdoor air temperature. In this case, 0% SHS is analogous to 100% GAE or 100% AIE. As SHS is a single percentage that represents the whole model, it is ideally suited to be displayed on a temporal map, in which case 0% SHS would be yellow, fading towards red for 100% Solar Heat Surplus and towards blue for negative 100% Solar Heat Scarcity. Although it may seem that 0% SHS is a transition point from cooling to heating and would rarely occur, it must be recalled that there are often several degrees between the cooling and heating set points, making that transition area broader than it might initially appear.

Although it might be viable to display the change of the effect of solar heat gain throughout the day if the input data are reliable enough over the day, with this simplified calculation method it makes more sense to look at balance point data in terms of a daily total energy load sum. This could be seen as a thermal balance potential for the day, in the sense that a similarity between the heating and cooling loads for a particular day could result in comfortable indoor temperatures with the proper deployment of thermal mass. The resulting daily total SHS then indicates an overbalance towards heating (bluish) or cooling (reddish) during the day, and is represented as a solid vertical stripe

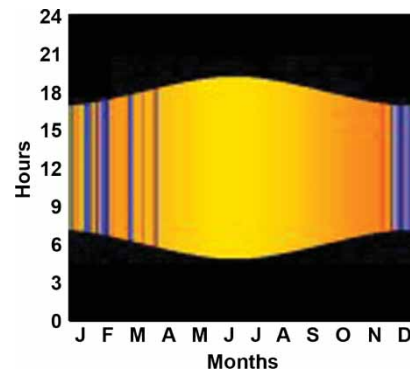


**Figure 18** Solar heat scarcity/surplus temporal map displayed in the form of daily totals

on the temporal map. Figure 18 illustrates this concept and reveals occasional scarcity of gains in the winter (blue), a slight excess (surplus) in the autumn (orange-red) and a proper balance in the summer. The result is thus a look at seasonal, rather than hourly, trends of SHS, but it is more representative of the accuracy of the data involved in balance point calculations.

### Comprehensive analysis and applicability to practice

A hospital room model is used to demonstrate what type of conclusions can be drawn from temporal graphics and how the new metric forms described above can



inform design decisions. The perspective of actual users of the proposed approach is discussed thereafter.

### Three-faceted goal-based analysis

Design involves a great many choices, and the most informed way to make choices is often by comparing options. The presented example will examine the use of temporal maps to compare orientation and shading options for a single room. This example was inspired by previous work on daylight in healthcare facilities (Pechacek *et al.*, 2008). The model proportions conform to healthcare codes: the main part of the room is 4.9 m wide  $\times$  4 m deep; and the bed, which has a clearance of at least 0.9 m on each side, is 2.4  $\times$  1.0  $\times$  0.94 m. The ceiling reflectance is 80%; wall reflectance is 60%; floor reflectance is 30%; and visible transmittance of the window is 73% and is meant to represent double-pane low-e glass (Figure 19). The location of this model is Phoenix in Arizona, and several orientations of this room were studied.

When designing a daylighting scheme focused on health and recovery, the most interesting light levels are those at the patient's face, both sitting and lying down. It has been found that humans must be exposed to certain amounts of light to regulate their endogenous circadian rhythms and maintain a healthy hormonal balance (Rea *et al.*, 2002; Cajochen *et al.*, 2000; Küller and Lindsten, 1992). As a preliminary investigation of the connection between non-visual light effects and façade design, Pechacek *et al.* (2008) used the night-time findings by Cajochen *et al.* (2000) to determine a daylight exposure threshold of 192 lux for alertness. Therefore, the goal here is to keep the light on the patient's face above 192 lux (with no partial credit buffer) during daytime. In terms of upper threshold, a value of 2000 lux was set. This is based on the same criteria as for the example explained above, *i.e.* minimizing the risk of being exposed to excessive contrasts (especially direct sun in one's eyes). Simulations were done with the LSV engine (cf. the second section) for three orientations – south, east and west – with two shading options – no shading and fixed horizontal louvres.

The values used in the balance point equation were all derived using American Society of Heating, Refrigerating and Air-Conditioning Engineers (ASHRAE) standards and values taken from the Hospital model in the DOE set of 16 commercial benchmark buildings (ASHRAE, 2001; Torcellini *et al.*, 2008). The  $U$ -values of the exterior walls and windows were 0.856 ( $W/m^2 K$ ) and 3.24 ( $W/m^2 K$ ), respectively; the Solar Heat Gain Coefficient (SHGC) or  $g$ -value of the glass was 0.60, which is the SHGC ( $g$ -value) of a good double-glazed, low-e window glass according to ASHRAE (2001); and the total ventilation rate was 0.1 ( $m^3/s$ ).

The occupancy rate was 0.1 (people/ $m^2$ ); and 130 W was used to represent the heat gain of a human. The general equipment heat gain assumption was 500 (W); and the occupancy was assumed to be continuous with 72°F (22.2°C) and 69°F (20.6°C) as the cooling and heating set-point temperatures respectively.

The temporal maps illustrating the AIE and GAE at the patient's face are shown in Figures 20a and 20b for a patient who is lying down. SHS temporal maps created using daily load totals are shown in Figure 20c. The horizontal louvres in this example are fixed, wider-spaced permanent louvres rather than Venetian blinds.

From these maps, it can be observed that for the reclining patient in the option without shades, the illuminance stays greater than 192 lux nearly all the time for all orientations (with the west slightly outperforming the south, which slightly outperforms the east in the evening). Correlating glare problems can also be seen for all orientations (that correspond to the periods of the day and year where excessive illuminance levels were detected, which is comforting in terms of metrics reliability): in the summer mid-morning in the east-facing room, in the winter mid-day in the south-facing room, and in a large portion of sunset times in the west-facing room. If fixed horizontal louvres are added, there is a reduction, but not elimination, of glare for the reclining patient, and all orientations gain times when the patient is not receiving enough light. The south-facing room still maintains good illuminance levels in the winter, but both east and west drop too low in the afternoons and mornings, respectively.

Taking the SHS maps into account (Figure 20c) is another point in favour of including horizontal louvres. Although the balance point is not really accurate enough to identify hourly problems in solar energy influx, the SHS maps bear out the previous seasonal conclusions – the unshaded south-facing room incurs more solar gain when the sun is more normal to the windows in the winter, and Phoenix has a hot enough climate so that the solar gain is still an issue in the cooler months. The east- and west-facing unshaded rooms have problems with excess solar energy throughout most of the year, and this problem is slightly greater for the east-facing window than for the west. When all orientations are shaded by horizontal louvres, the excess solar gain is largely mitigated, although this is done to the detriment of desirable illuminance. Unsurprisingly, the horizontal louvres cut out slightly more solar gain on the south-facing orientation.

It is obvious from this example that the horizontal shades help the space avoid glare and excessive solar heat gain, but at the cost of some useful illuminance. The differences in east- and west-facing illuminance

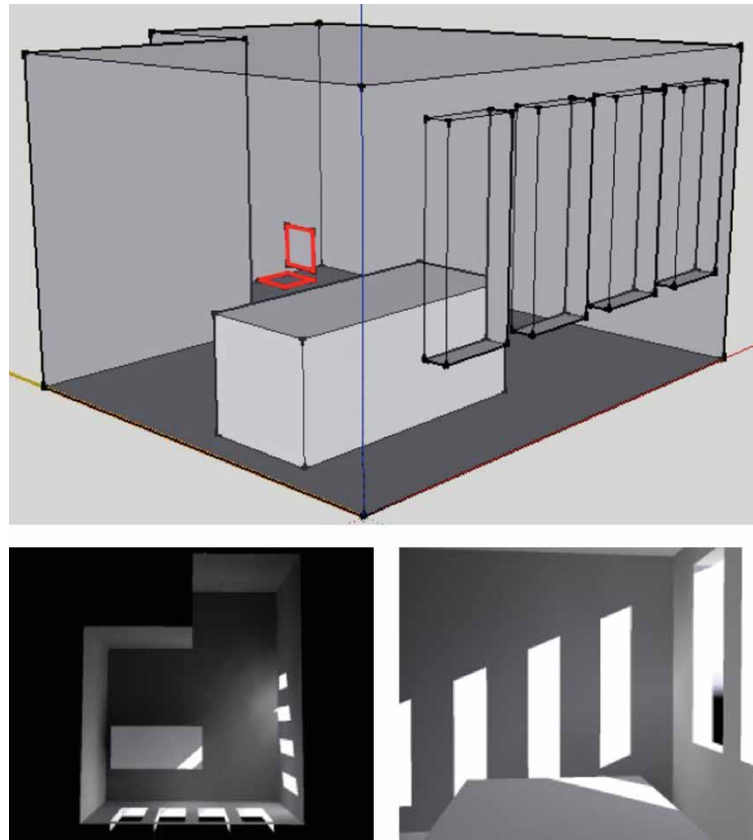


**Figure 19** Sketch-up model and several renderings of the hospital room. The sensor planes are outlined in red

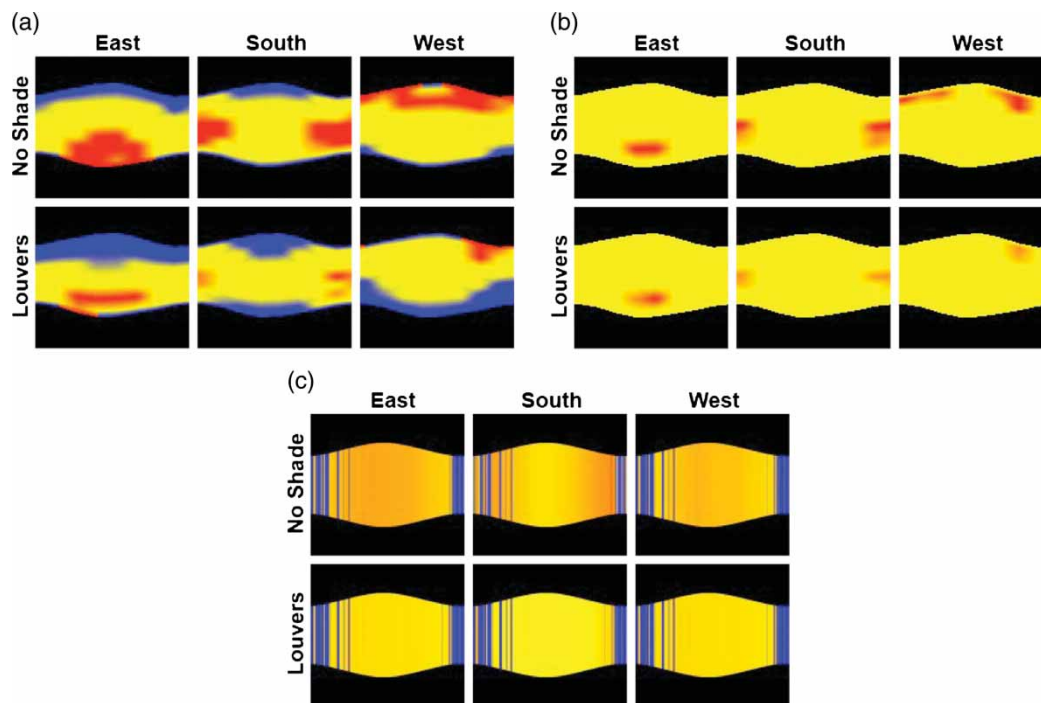


**Figure 20** Series of temporal maps showing (a) AIE, (b) GAE and (c) SHS for different orientations and shading strategies for a hospital room in Phoenix in Arizona, US

and glare behaviour are largely due to the fact that the bed is on one side of the room. Given all three sets of data, the trade-off between maintaining illuminance levels and lowering both glare and unwanted solar heat gain (given the Phoenix climate) can be quantified as periods when the room is suboptimal. The architect could use similar comparisons to choose the best shading system for the climate and orientation, and to design a higher number of patient recovery rooms with the best-performing orientations. Strategies can also be suggested involving the timing and control of automatic blinds, moving the beds or filling the best rooms first according to the time of year.

#### Application in architectural studies

The proposed goal-based framework has by now been applied in different contexts. This allows a discussion of its limitations and adequacy in providing useful design support.

A pair of preliminary user surveys were conducted in 2009 at Massachusetts Institute of Technology (MIT), where Lightsolve was initially developed as a tool. The first was given to practitioners and students attending a daylighting design workshop, where they were taught to use both Lightsolve and Ecotect (with exports to Radiance and Daysim through a workflow similar to that given by Reinhart and Wienold, 2010). The aim of this survey was to help validate the usefulness of Lightsolve's temporal approach and the intuitive nature of the temporal maps, and to observe architects' interaction with the software. It was complemented by a stand-alone survey conducted with architecture students on comparing spatial and temporal daylighting data to judge how intuitive temporal data were to the inexperienced architect. These pilot studies showed that the temporal format and the goal-based colour scale were usable and useful in a design process, and of similar effectiveness at improving the designer's understanding of daylighting performance as traditional approaches (Kleindienst and Andersen, 2009b). A more extensive study was then conducted on students, researchers and practitioners with Lightsolve to test its Expert System (Gagne *et al.*, 2011), focused on the impact it might have in an actual design exercise. The results were particularly encouraging in that it showed a significant educational potential for the tool as well as a good response from participants in terms of interest to use it in practice.

Apart from these controlled studies, Lightsolve has been tested since 2009 in class contexts (mostly at MIT and the Ecole Polytechnique Fédérale de Lausanne (EPFL)) and professional workshops (*e.g.* Lightfair International in 2010), as well as in consulting projects (most notably for a building extension

including lightwells of multiple stories). Precious feedback has also been gathered from researchers from other universities who have used the tool for their own research purposes (Piderit *et al.*, 2011; Pellegrino *et al.*, 2011). These various applications confirmed that such time-focused, comprehensive goal-based metrics had a significant potential for interactivity in the early stages of design and could be interesting complements to the more traditional spatial grids and annual summaries.

#### Conclusions

Daylighting analysis is underused in the earliest stages of design, precisely the time at which it could do the most good. There may be several reasons for this, including the current design culture and educational practices, but there is currently a lack of interactive yet comprehensive design analysis methods that give the architect all necessary information in a form that is clear and concise.

The issues of pre-processing and presentation of usable daylighting data were considered for the purpose of making good design decisions in the earliest stage of daylighting design. Three goal-based metrics are proposed to enable the designer to understand the daylighting performance of a space in terms of illuminance (Acceptable Illuminance Extent), glare (Glare Avoidance Extent), and solar heat gain (Solar Heat Surplus/Scarcity) simultaneously. Each metric was developed to be readable in a temporal graphic format and comparable with other goal-based metrics through an original, non-linear colour scale that expresses how closely goals are being fulfilled in a consistent and refined way (*e.g.* indicating combined occurrence of too high and too low light input).

The most important objective of this paper is not only the formulation of goal-based metrics for daylighting design, but also to bring and evaluate the three most critical aspects of daylighting performance together: illumination, glare and overheating. A consistent format was created that places the focus both on their relationship with daily and seasonal variations (which have fundamental implications on early stage design decisions), and on performance objectives the designer actually wants to reach. The ability to understand at a glance how they complement and contradict each other is particularly critical when choices and tradeoffs must be made between conflicting objectives. This challenge, very relevant to daylighting and present in almost every architectural design process, led to a parallel research effort of incorporating the approach described here into a guided, iterative search for improved performance based on multiple goals, that takes shape as an interactive

expert system (Gagne and Andersen, 2011; Gagne et al., 2011).

While some of the components of these data-processing and display methodologies have been in existence for years, it is their unique combination in a consistent, intuitive and visual format that holds great promise in the capacity of helping architects to make design decisions at the early stages of design, with a focus on daily and seasonal variations.

## Acknowledgements

The authors were supported by the Massachusetts Institute of Technology and the Martin Family Society of Fellows for Sustainability. M. Andersen was also supported by the Ecole Polytechnique Fédérale de Lausanne. The authors would like to thank Leslie Norford, Christoph Reinhart and Jan Wienold for their constructive input.

## References

- American Society of Heating, Refrigeration, and Air-Conditioning Engineers (ASHRAE) (2001) *ASHRAE Handbook, Fundamentals*, ASHRAE, Atlanta, GA.
- Andersen, M., Gagne, J.L. and Kleindienst, S. (2011) Informing well-balanced daylight design using Lightsolve, in *Proceedings of the CISBAT 11 Conference*, Lausanne, Switzerland, 14–15 September 2011.
- Andersen, M., Kleindienst, S., Yi, L., Lee, J., Bodart, M. and Cutler, B. (2008) An intuitive daylighting performance analysis and optimization approach. *Building Research & Information*, 36(6), 593–607.
- Bourgeois, D., Reinhart, C.F. and Ward, G. (2008) A standard daylight coefficient model for dynamic daylighting simulations. *Building Research & Information*, 36(1), 68–82.
- Boyce, P.R., Hunter, C. and Howlett, O. (2003) The benefits of daylight. Literature Review Report, Lighting Research Center, Rensselaer Polytechnic Institute, Troy NY, Sponsored by Capturing the Daylight Dividend Program.
- Brainard, G.C., Hanifin, J.P., Greeson, J.M., Byrne, B., Glickman, G., Gerner, E. and Rollag, M. (2001) Action spectrum for melatonin regulation in humans: evidence for a novel circadian photoreceptor. *Journal of Neuroscience*, 21(16), 6405–6412.
- Cajochen, C., Zeitzer, J.M., Czeisler, C.A. and Dijk, D.J. (2000) Dose–response relationship for light intensity and ocular and electroencephalographic correlates of human alertness. *Behavioral Brain Research*, 115, 75–83.
- Cannon-Brookes, S.W.A (1997) Simple scale models for daylighting design: analysis of sources of error in illuminance prediction. *Lighting Research and Technology*, 29(3), 135–142.
- Commission Internationale de l'Éclairage (CIE) (1994) *Spatial Distribution of Daylight – Luminance Distributions of Various Reference Skies*. Publ. No. 110–1994, CIE, Vienna.
- Cutler, B., Sheng, Y., Martin, S., Glaser, D. and Andersen, M. (2008) Interactive selection of optimal fenestration materials for schematic architectural daylighting design. *Automation in Construction*, 17(7), 809–823.
- de Groot, E., Zonneveldt, L. and Paule, B. (2003) Dial Europe: a decision support tool for early lighting design, in *Proceedings of the 8th International IBPSA Conference*, Eindhoven, the Netherlands, 11–14 August 2003.
- Edwards, L. and Torcellini, P.A. (2002) *A Literature Review of the Effects of Natural Light on Building Occupants*, National Renewable Energy Laboratory Golden, CO.
- Gagne, J.M.L. and Andersen, M. (2011) A daylighting knowledge-base for performance-driven facade design exploration. *LEUKOS – Journal of the Illuminating Engineering Society of North America*, 8(2), 93–101.
- Gagne, J.M.L., Andersen, M. and Norford, L.K. (2011) An interactive expert system for daylighting design exploration. *Building and Environment*, 46(11), 2351–2364.
- Galasiu, A.D. and Reinhart, C.F. (2008) Current daylighting designing practice: a survey. *Building Research & Information*, 36(2), 159–174.
- Glaser, D.C. and Ubbelohde, M.S. (2001) Visualization for time dependent building simulation, in *Proceedings of the 7th International IBPSA Conference*, Rio de Janeiro, Brazil, 13–15 August 2001.
- Glaser, D.C. and Ubbelohde, M.S. (2002) Techniques for managing planar daylight data. *Building and Environment*, 64, 825–831.
- Heschong, L., Wright, R.L. and Okura, S. (2002) Daylighting impacts on human performance in school. *Journal of the Illuminating Engineering Society*, 31(2), 101–111.
- Heschong-Mahone Group, Inc (2003) *Windows and Classrooms: A Study of Student Performance and the Indoor Environment*, Fair Oaks CA, California Energy Commission.
- Hui, S.C.M. (1997) , , Overall thermal transfer value (OTTV): how to improve its control in Hong Kong, in *Proceedings of the One-day Symposium on Building, Energy, and Environment*, Hong Kong, China, 16 October 1997, pp. 12-1–12-11.
- Ihm, P., Nemri, A. and Krarti, M. (2009) Estimation of lighting energy savings from daylighting. *Building and Environment*, 44(3), 509–514.
- Kleindienst, S. and Andersen, M. (2009a) The adaptation of daylight glare probability to dynamic metrics in a computational setting, in *Proceedings of the Lux Europa 2009 Conference*, Lausanne, Switzerland, 9–11 September 2009.
- Kleindienst, S. and Andersen, M. (2009b) User assessment of a new interactive graphical visualization for annual daylighting analysis, in *Proceedings of the CISBAT 2009 Conference*, Lausanne, Switzerland, 2–3 September 2009.
- Kleindienst, S. and Andersen, M. (2010) Solar heat surplus and solar heat scarcity: the inclusion of solar heat gain in a dynamic and holistic daylight analysis, in *Proceedings of SimBuild 2010*, New York, NY, US, 11–13 August 2010.
- Kleindienst, S., Bodart, S. and Andersen, M. (2008) Graphical representation of climate-based daylight performance to support architectural design. *LEUKOS – Journal of the Illuminating Engineering Society of North America*, 5(1), 39–61.
- Küller, R. and Lindsten, C. (1992) Health and behavior of children in classrooms with and without windows. *Journal of Environmental Psychology*, 12, 305–317.
- Lockley, S.W., Evans, E.E., Scheer, F.A., Brainard, G.C., Czeisler, C.A. and Aeschbach, D. (2006) Short-wavelength sensitivity for the direct effects of light on alertness, vigilance, and the waking electroencephalogram in humans. *Sleep*, 29(2), 161–168.
- Mardaljevic, J. (2004) Spatio-temporal dynamics of solar shading for a parametrically defined roof system. *Energy and Buildings*, 36(8), 815–823.
- Mardaljevic, J. (2009) Application of the useful daylight illuminance metric: a parametric evaluation covering 480 combinations of building type, climate and orientation, in *Proceedings of Lux Europa 2009*, Istanbul, Turkey, 9–11 September 2009.
- Mardaljevic, J. and Nabil, A. (2006) The useful daylight illuminance paradigm: a replacement for daylight factors. *Energy in Buildings*, 38(7), 905–913.

- Pechacek, C.S., Andersen, M. and Lockley, S.W. (2008) Preliminary method for prospective analysis of the circadian efficacy of (day)light with applications to healthcare architecture. *LEUKOS – Journal of the Illuminating Engineering Society of North America*, 5(1), 1–26.
- Pellegrino, A., Lo Verso, V.R.M. and Cammarano, S. (2011) Limits and potentials of different daylighting design approaches based on dynamic simulations, in *Proceedings of the CISBAT 2011 Conference*, Lausanne, Switzerland, 14–15 September 2011.
- Perez, R., Michalsky, J. and Seals, R. (1992) Modeling sky luminance angular distribution for real sky conditions: experimental evaluation of existing algorithms. *Journal of the Illuminating Engineering Society*, 21(2), 84–92.
- Piderit, B., Bodart, M. and Norambuena, T. (2011) A method for integrating visual comfort criteria in daylighting design of school, in *Proceedings of the PLEA 2011 Conference on Passive and Low Energy Architecture*, Louvain-la-Neuve, Belgium, 13–15 July 2011.
- Rashid, M. and Zimring, C. (2008) A review of the empirical literature on the relationships between indoor environment and stress in health care and office settings: problems and prospects of sharing evidence. *Environment and Behavior*, 40(2), 151–190.
- Rea, M.S. (ed.) (2000) *The IESNA Lighting Handbook: Reference and Application*, 9th edn, Illuminating Engineering Society of North America (IESNA), New York, NY.
- Rea, M.S., Figueiro, M.G. and Bullough, J.D. (2002) Circadian photobiology: an emerging framework for lighting practice and research. *Lighting Research and Technology*, 34(3), 177–190.
- Reinhart, C.F. (2005) *Tutorial on the Use of Daysim/Radiance Simulations for Sustainable Design*. 8 February, National Research Council of Canada, Institute for Research in Construction, Ottawa, ON.
- Reinhart, C.F. and Fitz, A. (2004) Key findings from an online survey in the use of daylight simulation programs, in *Proceedings of eSim 2004*, Vancouver, BC, Canada, 10–11 June 2004, pp. 1–8.
- Reinhart, C.F. and Fitz, A. (2006) Findings from a survey on the current use of daylight simulations in building design. *Energy and Buildings*, 38(7), 824–835.
- Reinhart, C.F. and Walkenhorst, O. (2001) Validation of dynamic RADIANCE-based daylight simulations for a test office with external blinds. *Energy and Buildings*, 33, 683–697.
- Reinhart, C.F. and Wienold, J. (2010) The daylighting dashboard – a simulation-based design analysis for daylight spaces. *Building and Environment*, 46(2), 386–396.
- Reinhart, C.R., Bourgeois, D., Dubrous, F., Laouadi, A., Lopez, P. and Stelescu, O. (2007) Daylight 1-2-3 – a state-of-the-art daylighting/energy analysis software for initial design investigations, in *Proceedings of the 10th International IBPSA Conference*, Beijing, China, 3–6 September 2007, pp. 1669–1676.
- Rogers, Z. (2006) *Daylighting Metric Development using Daylight Autonomy Calculations in the Sensor Placement Optimization Tool: Development Report and Case Studies*. 17 March, Architectural Energy Corporation, Boulder, CO (available at: <http://www.archenergy.com/SPOT/download.html>) (accessed July 2010).
- Sarawgi, T. (2006) Survey on the use of lighting design software in architecture and interior design undergraduate education. *International Journal of Architectural Computing*, 4(4), 91–108.
- Saxena, M., Hescong, L., Van Den Wymelenberg, K. and Wayland, S. (2010) 61 Flavors of daylight, in *American Council for an Energy Efficient Economy, Summer Study Conference Proceedings*.
- Swiss Federal Office of Energy (2009) *Energieforschung 2009 – Ueberblicksberichte*, Bern, Swiss Confederation.
- Thanachareonkit, A., Scartezini, J.L. and Andersen, M. (2005) Comparing daylighting performance assessment of buildings in scale models and test modules. *Solar Energy*, 79, 168–182.
- Torcellini, P., Deru, M., Griffith, B., Benne, K., Halverson, M., Winiarski, D. and Crawley, D.B. (2008) DOE commercial building benchmark models, in *Proceedings of the 2008 ACEEE Summer Study on Energy Efficiency in Buildings*, Pacific Grove, CA, US, 17–22 August 2008 (available at: <http://www.nrel.gov/docs/fy08osti/43291.pdf>) (accessed on October 2009).
- Tregenza, P.R. and Waters, I.M. (1983) Daylight coefficients. *Lighting Research and Technology*, 15(2), 65–71.
- US Green Building Council (USGBC), Washington DC (2009) *LEED 2009 for New Construction and Major Renovation*, USGBC, Washington, DC (available at: <http://www.usgbc.org/ShowFile.aspxDocumentID=5546>) (accessed July 2010).
- Ubbelohde, M.S. (1998) Comparative evaluation of four daylighting software programs, in *Proceedings of ACEE Summer Study on Energy Efficiency in Buildings*, Panel 3, Paper 27, Pacific Grove, CA, 23–28 August, 1998.
- Urban, B.J. and Glicksman, L.R. (2007) A simplified rapid energy model and interface for nontechnical users, in *Proceedings of Oak Ridge National Laboratory, Buildings Conference X*, 2007.
- Utzinger, M. and Wasley, J.H. (1997) *Building Balance Point, Vital Signs Curriculum Materials Project*. August, University of California – Berkeley, and University of Wisconsin – Milwaukee (available at: <http://arch.ced.berkeley.edu/vitalsigns/res/rps.html>) (accessed October 2009).
- Veitch, J.A. (2005) Light, lighting, and health: issues for consideration. *LEUKOS – Journal of the Illuminating Engineering Society of North America*, 2(2), 85–96.
- Ward, G. (1998) *gensky.c. C code for Radiance Simulation Program Sky Generation*. Lawrence Berkeley Laboratory (available at: <http://radsite.lbl.gov/radiance/>) (accessed November 2009).
- Webb, A.R. (2006) Considerations for lighting in the built environment: non-visual effects of light. *Energy and Buildings*, 38, 721–727.
- Wienold, J. (2009) Dynamic daylight glare evaluation, in *Proceedings of the 11th International IBPSA Conference*, Glasgow, UK, 27–30 July 2009, pp. 944–951.
- Wienold, J. and Christoffersen, J. (2006) Evaluation methods and development of a new glare prediction model for daylight environments with the use of CCD cameras. *Energy and Buildings*, 38, 743–757.
- Winkelmann, F. and Selkowitz, S. (1985) Daylighting simulation in the DOE-2 building energy analysis program. *Energy and Buildings*, 8, 271–286.